EVIDENCE FOR ABSORPTION DUE TO HIGHLY-IONIZED GAS IN THE RADIO-QUIET QUASAR PG 1114+445

I.M. George [1,2], K. Nandra[1,3], A. Laor [4], T.J. Turner [1,2], F. Fiore[5,6], H. Netzer [7], R.F. Mushotzky[1]

ABSTRACT

We present results on the X-ray spectrum of the quasar PG 1114+445 from an *ASCA* observation performed in 1996 June, and a *ROSAT* observation performed 3 years earlier. We show good agreement between all the datasets can be obtained if the underlying continuum in the 0.2–10 keV band is assumed to be a powerlaw (photon index $\Gamma \simeq 1.8$) absorbed by photoionized material. The ionized gas imprints deep absorption edges in the observed spectrum $\lesssim 2$ keV due to OVII and OVIII, from which we determine its column density ($\sim 2 \times 10^{22}$ cm^{-2}) and ionization parameter ($U_X \sim 0.1$) to be similar to that observed in Seyfert-I galaxies. Unfortunately these data do not allow any strong constraints to be placed on the location, or solid angle subtended by the material at the ionizing source. We also find evidence for absorption in the Fe K-shell band in excess of that predicted from the lower energy features. This implies an Fe/O abundance ratio ~ 10 times the cosmic value, or an additional screen of more-highly ionized gas, possibly out-flowing from the nucleus. We briefly compare our results with those obtained from other active galaxies.

Subject headings: galaxies:active – galaxies:nuclei – galaxies:Seyfert – X-rays:galaxies – quasars: individual (PG 1114+445)

[1]Laboratory for High Energy Astrophysics, Code 660, NASA/Goddard Space Flight Center, Greenbelt, MD 20771

[2]Universities Space Research Association

[3]NAS/NRC Research Associate

[4]Physics Department, Technion, Haifa 32000, Israel

[5]Osservatorio Astronomico di Roma, via dell'Osservatorio 5, Monteporzio-Catone (RM), I-00040, Roma, Italy

[6]SAX Scientific Data Centre, via corcolle 19, I-00131, Roma, Italy

[7]School of Physics and Astronomy and the Wise Observatory, The Beverly and Ramond Sackler Faculty of Exact Sciences, Tel Aviv University, Tel Aviv 69978, Israel.

1. INTRODUCTION

A number of *ROSAT* and *ASCA* X-ray observations of low luminosity Active Galactic Nuclei (AGN) have shown clear evidence for absorption by highly-ionized gas along the line-of-sight (e.g. Nandra & Pounds 1992; Turner et al 1993; Reynolds 1997; George et al 1997 and references therein). The presence of such gas is revealed primarily by the OVII and OVIII absorption edges imprinted on the underlying continuum. Recent studies show that the ionized gas generally has a relatively large column density (corresponding to effective hydrogen column densities $N_H \sim 10^{21}$–10^{23}cm^{-2}, although there are obvious selection effects due the bandpasses and sensitivities of the instruments), and exists in $\sim$ 50–75% of Seyfert-I galaxies (Reynolds 1997; George et al 1997, thereafter G97).

The situation in the case of higher-luminosity AGN is less clear. Recent studies have shown that a large fraction of radio-loud quasars (RLQs) show evidence for intrinsic absorption (Cappi et al 1997). The ionization state of the material generally cannot be determined from current data, although there is strong evidence that it is highly ionized in at least two cases (3C 351, Fiore et al 1993; 3C 273, Grandi et al 1997). Interestingly, intrinsic absorption appears to be far less common in radio-quiet quasars (RQQs), which are thought to make up $\sim$90% of total quasar population (Laor et al 1997; Fiore et al 1997). Indeed there is only two cases documented to-date: MR 2251-178 (Halpern 1984, Pan, Stewart & Pounds 1990, Mineo & Stewart 1993) and IRAS 13349+2438 (Brandt, Fabian & Pounds 1996). Such a difference between the two classes could be taken to mean that gas does not exist along the line–of–sight in RQQs. Alternatively, a substantial column density of gas could be present, but so highly ionized to be transparent in the X-ray band, or that the absorption features imprinted by such gas could be swamped by continuum photons arriving via another (transparent) travel-path.

PG 1114+445 ($z = 0.144$; Schmidt & Green 1983) is a RQQ with $L_{IR} \sim L_{UV} \simeq 10^{45}$ erg s^{-1}, lying in a direction of relatively low Galactic line-of-sight column density ($N_{HI}^{Gal} = 1.94 \times 10^{20}$ cm^{-2} from the 21cm measurements of Murphy et al 1996). These characteristics led to the inclusion of the source as one of 23 quasars forming the complete sample of the Bright Quasar Survey, studied by the Position Sensitive Proportional Counter (PSPC) on *ROSAT* (Laor et al 1997). Interestingly, PG 1114+445 was one of the few objects whose PSPC spectrum could not be adequately modelled by a single power-law and the only object for which there was strong evidence for absorption by ionized material (Laor et al. 1994). Further evidence for absorption by ionized material comes from a recent *HST* observation which has revealed UV absorption lines at CIV, NV and Lyα (Mathur 1997). Here we present the results from a follow-up *ASCA* observation of PG 1114+445, along with a reanalysis of the PSPC data.

2. OBSERVATIONS AND DATA REDUCTION

The new observation reported here was performed using *ASCA* on 1996 May 06–07. The *ASCA* satellite (Makishima et al. 1996) consists of four identical, co-aligned X-ray telescopes (XRTs; Serlemitsos et al. 1995). Two solid-state imaging spectrometers (SIS0 and SIS1), each consisting of four CCD chips, sit at the focus of two of the XRTs, and provide coverage over the ∼0.4–10 keV band (Burke et al. 1994). Two gas imaging spectrometers (known as GIS2 and GIS3) sit at the focus of the other two XRTs, and provide coverage over the ∼0.8–10 keV band (Ohashi et al. 1996 and references therein). The observation reported here was carried out in `1-CCD` mode with the target in the nominal pointing position. The data collected in `FAINT` and `BRIGHT` telemetry modes were combined. We employed the same data selection criteria and data analysis methods for the *ASCA* data as presented in Nandra et al (1997a) using the `FTOOLS/XSELECT` package (v3.5 & 3.6). Combined, these gave rise to 5–7 $\times 10^4$ s of useful data in each of the detectors, from which we derive mean source count rates of $(4.5 \pm 0.1) \times 10^{-2}$ ct s^{-1} and $(3.4 \pm 0.1) \times 10^{-2}$ ct s^{-1} in the SIS0 and GIS2 detectors respectively, and similar rates in SIS1 and GIS3. The total number of source photons detected in each instrument was 2–3 $\times 10^3$. We find no significant variability on timescales $\lesssim 90$ min, and only marginal evidence changes in flux on longer timescales.

We have also independently analysed the *ROSAT* PSPC observation of PG 1114+445 presented by Laor et al. (1994), having obtained the data from the archive. This observation was carried out on 1993 Jun 06–07, and using standard data selection and reduction techniques gives rise to 7×10^3 s of useful data and a mean source count rate of $(10.2 \pm 0.4) \times 10^{-2}$ ct s^{-1}. No significant variability was observed.

A number of serendipitous sources are apparent within the field of view of *ROSAT*, at least one of which is also detected in the *ASCA* GIS, but at sufficiently large angular distances not to affect the analysis of PG 1114+445 presented here.

3. SPECTRAL RESULTS

Given the lack of strong variability during the observations, mean spectra were constructed for each detector, and it is the results from these that we concentrate on for the rest of the paper. As is common practice, in all cases we fit the data from each detector simultaneously, but allowing the normalization of each to be a free parameter to allow for differences in the sizes of the extraction cell used, along with any discrepancies in the absolute flux calibration of the individual telescope/detector systems. The spectral analysis

was performed using `XSPEC` (v9.01; Arnaud 1996). Appropriate detector redistribution matrices were used (those released 1994 Nov 09 and 1995 Mar 06 for the *ASCA* SIS and GIS respectively, and `pspcb_gain2_256.rmf` for the *ROSAT* PSPC). The effective area appropriate for each dataset was calculated using `ascaarf`[8](v2.5) for the *ASCA* data, and `pcarf`(v2.1.0) for the PSPC data. In the case of the SIS data, we have restricted our spectral analysis to energies ≥ 0.6 keV due to residual uncertainties in the calibration of the SIS/XRT instrument (see Dotani et al. 1996 and the information provided by the *ASCA* GOF at NASA/GSFC[9]). However, whilst the calibration is suspect at these energies, it is considered unlikely to be in error by $\gtrsim 20\%$. Thus, following G97 we have also calculated the weighted mean of the data/model residuals ($\overline{R_{0.6}}$), when the best-fitting model is extrapolated below 0.6 keV. The rationale behind this parameter is that it allows us to identify models, which are deemed acceptable > 0.6 keV, but in which the extrapolation to energies < 0.6 keV is inconsistent with the suspected size of the calibrations uncertainties.

The raw spectra extracted for each detector were grouped such that each resultant channel had at least 20 counts per bin, permitting us to use χ^2 minimization during the spectral analysis. This results in a total of 511 spectral bins for the combined *ASCA* detectors, and 37 spectral bins for the PSPC data. In passing, we note that in the 0.6-0.8 keV band these grouped spectral bins are each typically 0.06 keV wide (for both the SIS and PSPC datasets). This is comparable to the spectral resolution of the SIS at the epoch of the observations (FWHM $\simeq 0.09$ keV) and far smaller than the spectral resolution of the PSPC (FWHM $\simeq 0.35$ keV) within this energy band. Appropriate background spectra were extracted from source-free regions of each detector.

We have compared a number of hypothetical models with the mean spectra. In all models considered here, we have assumed an underlying continuum represented by a single power-law (of photon index Γ) throughout the 0.1–10 keV band (observers frame). All the models also include the effects of absorption by neutral material at $z = 0$ parameterized by an effective hydrogen column density $N_{H,0}$ (assuming the abundances and cross-sections of Morrison & McCammon 1983), which can be allowed to vary during the spectral analysis (but constrained to be $\geq N_{HI}^{Gal}$). Most models include an additional column density $N_{H,z}$ of absorbing material at the redshift of the source. Errors are quoted at 68% confidence for the appropriate number of interesting parameters (where all free parameters are considered interesting except for the absolute normalization of the model).

---

[8]so as to include the Gaussian 'fudge', but not the filter 'fudge' in the case of the SIS datasets. We have also compared our results to those obtained using several developmental versions of `ascaarf` (up to and including v2.64), but find no significant differences.

[9] see `http://heasarc.gsfc.nasa.gov/docs/asca/cal_probs.html` for up-to-date information

3.1. Analysis of the overall continuum

3.1.1. Fits to the ASCA data

We find a simple power-law fit to the *ASCA* data in the 0.6–10 keV band confirms the presence of substantial absorption. If the absorbing material is assumed to be neutral we find $N_{H,0} \simeq 6 \times 10^{21}$ cm^{-2} or $N_{H,z} \simeq 7 \times 10^{21}$ cm^{-2} depending whether the material is assumed to be local or at the redshift of the quasar. Both fits gave a photon index $\Gamma \simeq 1.6$ and statistically acceptable fits (with reduced χ^2 value of $\chi^2_\nu = 1.0$). However the extrapolation of both best-fitting models predicts fewer counts < 0.6 keV than observed by a factor $\overline{R_{0.6}} \sim 14$, and give rise to an increase in χ^2-statistic of $\Delta\chi^2_{0.6} \sim 70$ (for 6 additional spectral bins). Such a discrepancy is far greater than can be accounted for remaining uncertainties in the instrumental calibration. As we shall see below, these solutions are artifacts of the presence of absorption by ionized gas.

Numerous elements have photoelectric absorption edges with threshold energies within the 0.6–1.0 keV band. However, for cosmic abundances, the opacity in this band is dominated by K-shell absorption by C, O and Ne, and L-shell absorption by Fe (e.g. Morrison & McCammon 1983). Given the redshift of PG 1114+445, the most significant edges likely to be observable in *ASCA* spectra are those due to OVII and OVIII, with rest–frame energies of 739 and 871 eV respectively. Including such edges in our analysis (fixing $N_{H,0} = N_{H,0}^{Gal}$ and $N_{H,z} = 0$), we find optical depths in these species of τ(OVII)$\simeq 2.5$ and τ(OVIII)$\simeq 1.1$. Such a model can be considered a crude parameterization of the absorption features imprinted by ionized gas along the line–of–sight to the nucleus. However, at such large optical depths absorption by other abundant elements is likely to be important also, hence a more detailed treatment is required. Here we consider the case where the material is ionized by the central continuum, and employ theoretical spectra generated using the photoionization code `ION` (Netzer 1993, 1996, version `ION95`). The ionization state of the gas is parameterized by the 'X-ray ionization parameter' U_X (Netzer 1996; where the ionizing radiation field is determined over the 0.1–10 keV band). Further details on the assumptions made in the `ION` models and the method by which they were included in the spectral analysis can be found in G97.

We find that including the absorption by photoionized gas provides an excellent description of the *ASCA* data (with $N_{H,0} = N_{HI}^{Gal}$), giving $\Gamma \simeq 1.8$, $N_{H,z} \simeq 2 \times 10^{22}$ cm^{-2} and $U_X \simeq 0.1$ (Table 1, line 1). The addition of U_X as an additional free parameter is significant at >99.9% confidence (F-statistic of 33.7). Furthermore this model gives far better agreement with the *ASCA* data < 0.6 keV ($\overline{R_{0.6}} \sim 0.8$, consistent with the current uncertainties in the instrumental calibration). When such a model is assumed,

we find $N_{H,0}$ consistent with N_{HI}^{Gal}, with an upper limit to any such excess absorption of $\Delta N_{H,0} \simeq 3 \times 10^{21}$ cm^{-2} (Table 1, line 2). The best-fitting model spectrum, along with the observed data/model ratios (for the $N_{H,0} = N_{HI}^{Gal}$ case) are shown in Fig 1, and the χ^2-contours in $N_{H,z}$–U_X space shown (solid lines) in Fig 2. As can be seen from Fig. 1, for the best fitting values of $N_{H,z}$ and U_X the intervening gas imprints a series of absorption edges on the underlying continuum, dominated by CVI, OVII and OVIII. However, it should be noted that the ionization level of the gas is such that it becomes increasingly transparent as one moves to lower energies below the OVII edge (0.65 keV in the observer's frame). It is this behaviour that leads to a better agreement between the extrapolated model and the observed SIS data < 0.6 keV, and we suggest, with the PSPC data (see below). We have considered models in which the ionized absorber attenuates only a fraction of the underlying continuum. However in all cases we find a covering-fraction consistent with 100%, thus such models are not considered further. Stringent constraints cannot be placed on the redshift of the ionized gas, z_{abs}, using the current data. However we do find $z_{abs} > 0.103$ at 90% confidence, consistent with the systemic redshift of the host galaxy, and limiting the ionized gas to be in an outflow/wind of velocity $\lesssim 10^4$ km s^{-1} relative to the nucleus[10].

With the assumption that our line-of-sight is not uniquely privileged, we have also tested whether any useful constraints can be obtained on the solid angle, Ω, subtended by such gas at the central continuum source from its expected emission/scattering spectrum. However, the inclusion of such a component in the spectral analysis (where $N_{H,z}$ and U_X of the emitting gas is the same as those for the absorbing gas) is inconclusive. We find an upper limit on the strength of such a component is that expected from a full shell of such material ($\Omega = 4\pi$) assuming it was irradiated by the continuum source with a luminosity a factor $\lesssim 8$ times greater than that derived from the observations. This is hardly surprising given that by far the bulk of the emission expected from ionized gas in this region of $N_{H,z}$, U_X parameter–space occurs below the OVII edge, and hence < 0.6 keV in the observer's frame.

3.1.2. Fits to the ROSAT data

Considering the PSPC data alone, we confirm the results of Laor et al (1994) that a single powerlaw does not provide an adequate description of the data (giving

[10]It should be noted that the spectral energy resolution of the *ASCA* SIS ($\Delta E/E \simeq 0.14$ at the epoch of the observations) prevents the velocity distribution of the ionized gas being constrained within $\sigma_v \lesssim 2 \times 10^4$ km s^{-1}

$\chi^2/dof = 59.5/35$), but that a statistically satisfactory fit can be obtained with the addition of a deep absorption edge. From our analysis, fixing $N_{H,0}$ at N_{HI}^{Gal}, we find a best fitting solution with an edge of optical depth $\tau = 3.5^{+1.7}_{-1.3}$ at an energy $E_z = 0.77^{+0.05}_{-0.06}$ keV (in the rest–frame of the quasar) imprinted on an underlying continuum with $\Gamma = 1.96^{+0.17}_{-0.17}$ and $\chi^2/dof = 23.1/33$. These values are in agreement with those found by Laor et al (1994; $\tau \simeq 3$ at $E_z \simeq 0.76$ keV), and with a blend of the OVII and OVIII edges found in the analysis of the *ASCA* data. Repeating the analysis, but assuming the photoionization models described above (with $N_{H,0} = N_{HI}^{Gal}$), we find $N_{H,z} = 37^{+41}_{-22} \times 10^{21}$ cm^{-2}, $U_X = 0.24^{+0.11}_{-0.14}$, and $\Gamma = 1.7^{+0.3}_{-0.3}$ with $\chi^2/dof = 22.7/33$. These values are in good agreement with those obtained from the *ASCA* data above. However, despite the fact that the PSPC provides some data at energies < 0.6 keV, the low signal-to-nose ratio of these data along with the relatively poor spectral resolution of the detector lead to few additional constraints on the state of the ionized gas being provided by the PSPC data alone.

3.1.3. Joint analysis of the ASCA and ROSAT data

Here we present the results from a joint analysis of both the *ASCA* and *ROSAT* datasets which may give better constraints on the properties of the ionized gas. As previously, the same spectral model is assumed for the data from each mission, but the normalization (only) of the underlying powerlaw is allowed to vary in order to allow for any intensity variations in the source over the 3 years between the observations.

As expected, statistically acceptable results are obtained with the photoionization model (Table 1 lines 3 & 4), with the flux during the *ROSAT* observation being a factor $\sim 90\%$ of that at the time of the *ASCA* observations. This is close to the accuracy of the the absolute flux calibration between the two instruments, so is not significant. It can be seen that the best-fitting parameters are also consistent with those derived when the *ASCA* and *ROSAT* data are considered individually. The χ^2-contours in $N_{H,z}$–U_X space assuming $N_{H,0} = N_{H,0}^{Gal}$ are also shown (dashed curves) in Fig 2. Allowing the redshift of the ionized gas to vary during the analysis we find $0.115 \leq z_{abs} \leq 0.217$ (at 90% confidence), again consistent with the systemic redshift of the host galaxy, and limiting the ionized gas to have a velocity $\lesssim \pm 2 \times 10^4$ km s^{-1} with respect to the nucleus. In passing, we note however, that the best-fitting models for this combined analysis do consistently overpredict the number of counts observed in SIS < 0.6 keV ($\overline{R_{0.6}} \sim 0.5$–$0.7$). This may simply be due to the residual uncertainties in the calibration of the SIS/XRT instrument at these energies, or be an artifact of fitting non-simultaneous datasets with different signal-to-noise ratios from instruments with very different energy resolutions. The strength of any emission component

is restricted to be that from a full shell of such material assuming it was irradiated by the continuum source with a luminosity a factor $\lesssim 1.5$ times that derived from the observations.

3.2. Results from the Fe K-shell band

The analysis presented in §3.1 did not take into account the potential presence of features in the 6–9 keV band (in the rest–frame of the quasar) due to Fe K-shell transitions. Indeed, the data/model residuals shown in Fig. 1 do show a deficit in this energy range. This absorption feature appears to be present in all 4 *ASCA* detectors, and can be modelled with an absorption edge of energy E_z^{abs} (in the rest–frame of the quasar) and optical depth τ (where $\tau \propto (E/E_z^{abs})^{-3}$ for energies $E \geq E_z^{abs}$ and zero elsewhere). Considering the *ASCA* data alone and fixing $N_{H,0} = N_{H,0}^{Gal}$, the addition of these two parameters results in an improvement of $\Delta\chi^2 = 9.2$, significant at $> 95\%$ confidence (F-statistic $= 4.9$). We find $\tau = 0.35^{+0.38}_{-0.29}$ and $E_z^{abs} = 7.25^{+0.42}_{-0.48}$ keV. The confidence contours in the E_z^{abs}–τ plane are shown in Fig. 3a, along with the corresponding edge energies for Fe K-shell absorption. It can be seen that the edge is consistent with FeI–FeXIX at 90% confidence for $\tau > 0.1$, assuming absorbing material in the rest–frame of the quasar. The best-fitting τ corresponds to an equivalent hydrogen column density of $\sim 10^{19}/A_{\rm Fe}$ cm^{-2} where $A_{\rm Fe}$ is the abundance of Fe relative to hydrogen. Thus, if the Fe feature is produced in the same material as is responsible for the O features observed $\lesssim 1$ keV discussed above ($N_{H,z} \simeq 2 \times 10^{22}$ cm^{-2}), then we require $A_{\rm Fe} \sim 5 \times 10^{-4}$, a factor ~ 10 greater than the most recent estimations of the 'cosmic' abundance (Anders & Grevesse 1989).

We note that a yet superior fit is obtained if the absorption feature is assumed to be 'notch'-shaped (a saturated line with vertical sides, and $\tau = \infty$ within), giving $\Delta\chi^2 = 18$ compared to the model with no absorption. The best-fitting notch has an equivalent width of 343^{+214}_{-205} eV (equivalent to one rebinned spectral bin) and is centered at an energy $7.76^{+0.16}_{-0.24}$ keV (in the rest–frame of the quasar; Fig.3b) Assuming this is indeed material in the rest–frame of the quasar, such an energy is consistent with resonance scattering by Ni $K\alpha$ (<NiXXVIII) and Fe $K\beta$ (>FeXX). Although both families of interactions include transitions with relatively large oscillator strengths ($\sim$ 0.7–0.8), both interpretations are problematic. In the former case, the cosmic abundance of Ni is far smaller than that for Fe ($A_{\rm Ni}/A_{\rm Fe} \simeq 0.04$) making such an interpretation unlikely due to the lack of corresponding features due to Fe at lower energies. In the latter case, resonance scattering by Fe $K\alpha$ will dominate that due to Fe $K\beta$ for ionization states >FeXVI, again making such an interpretation unlikely due to the lack such a feature in 6.4–6.9 keV band. An alternative explanation of the notch is that it is due to resonance scattering by Fe $K\alpha$, but that the

material is out–flowing ($\sim$ 0.1c for FeXXV) with respect to the rest-frame of the quasar. However, the instrumental and cosmic backgrounds start to become a noticeable fraction of the observed signal from PG 1114+445 in this observation above $\sim$ 6 keV. Given that both the SIS and GIS detectors contain background features in this region (e.g. Gendreau 1994; Makishima et al. 1996), we consider the form of the absorption to require confirmation before more detailed interpretations can be made.

Emission features due to Fe K-shell processes are common in low luminosity AGN (e.g. Nandra & Pounds 1994), and have been claimed in high luminosity AGN (e.g. Williams et al. 1992; Nandra et al 1996). With such a deep Fe absorption in our spectrum, we might expect to observe the associated Kα emission. For the ionization levels suggested by the above fits including an edge (<FeXX) the emission line energy should be close to 6.4 keV. We have tested for the presence of such a line by adding a narrow Gaussian line to the model at that energy. Although a significant improvement is not obtained, the equivalent width $W_{K\alpha} = 60^{+120}_{-60}$ eV is consistent with the predictions of photoionization models assuming full coverage of the column density implied by the edge fits. If the emission line is broad, as observed in Seyfert 1 galaxies, then the upper limit to $W_{K\alpha}$ is larger by a factor ~ 5.

4. DISCUSSION AND CONCLUSIONS

In the previous section we have shown that both the *ASCA* and *ROSAT* spectra from PG 1114+445 are consistent with a single powerlaw continuum with $\Gamma \simeq 1.8$ absorbed by a column density of $\simeq 2 \times 10^{22}$ cm^{-2} of photoionized gas $U_X \simeq 0.1$. We suggests this offers the most plausible explanation of the the X-ray spectrum of this source, making it only the fifth quasar (alongside MR 2251-178, 3C 351, 3C 273 and IRAS 13349+2438) in which ionized material has been detected along the line–of–sight. After correcting for absorption (i.e. setting $N_{H,0} = N_{H,z} = 0$), the X-ray luminosities[11] are $L_X \simeq 5.7 \times 10^{44}$ erg s^{-1} and 2.7×10^{44} erg s^{-1} over the 0.1–10 keV and 2–10 keV bands (source-frame) respectively. This is comparable to the higher-luminosity examples of the sources considered by G97. Unfortunately these data do not allow any strong constraints to be placed on the location, or solid angle subtended by the ionized material at the ionizing source.

Clearly a comparison between the properties of the material dominating the absorption in the X-ray band of PG 1114+445 with that responsible for the absorption features seen in the UV might be revealing. To this end, in Table 2 we list the column densities of the abundant Li-like ions predicted from our best-fit model from §3.1. It should be stressed that

[11]assuming $H_0 = 50$ km s^{-1} Mpc^{-1} and $q_0 = 0.5$

such predictions are very sensitive to form of the ionizing continuum in the XUV band, and of course the elemental abundances. The values quoted in Table 2 assume the 'weak IR' continuum described by Netzer (1996), namely a *photon* index $\Gamma_o = 1.5$ in the optical/UV band from 1.6–40.8 eV, an index $\Gamma = 1.9$ in the X-ray band from 0.2–50 keV, and a powerlaw continuum in the XUV band connecting the fluxes at 40.8 eV and 0.2 keV, such that the ratio of the fluxes at 250 nm and 2 keV is $f_{250}/f_{2\rm keV} = 8.1 \times 10^3$ (corresponding to an optical–to–X-ray *energy* index $\alpha_{ox} = 1.5$). Following Netzer (1996), we assume undepleted 'cosmic abundances' (with (He, C, N, O, Ne, Mg, Si, S, Fe)/H = (10^3, 3.7, 1.1, 8, 1.1, 0.37, 0.35, 0.16, 0.4)/10^{-4}). For comparison, the column densities in the bound–free transitions in OVII & OVIII are 9.6×10^{18} cm^{-2} & 5.1×10^{18} cm^{-2} respectively. In passing we note that given the cross-sections for these transitions (2.4×10^{-19} cm^2 & 9.9×10^{-20} cm^2 respectively), the predicted optical-depth of OVII ($\tau \simeq 2.5$) is in good agreement with that obtained in §3.1.1 when the data is modelled as a powerlaw plus OVII & OVIII absorption edges. However, the observed optical-depth of OVIII ($\tau \simeq 1.1$) is a factor ∼2 larger than that predicted in our full photoionization calculations, primarily as a result of the modelled optical-depth of OVIII having to include the additional opacity due to Fe *L*-shell and NeIX *K*-shell transitions during the fitting process.

The parameters for the ionized gas obtained here for PG 1114+445 are very similar to those found for Seyfert-I galaxies. G97 find the ionization parameter typically clusters around $U_X \sim 0.1$ with column densities in the range $N_{H,z} \sim 10^{21}$–10^{23} cm^{-2}. The underlying spectral index also lies in the range found in Seyfert-I galaxies. The underlying continuum could not be determined unambiguously from the *ROSAT* PSPC data from the RLQ 3C 351 ($z = 0.371$, $L_X \simeq 3 \times 10^{45}$ erg s^{-1}). However the fits including absorption by ionized material reported by Fiore et al (1993) indicate a similar column density ($N_{H,z} \sim 1$–4×10^{22} cm^{-2}) to that found in PG 1114+445 and Seyfert-Is, but that the gas is less ionized ($U_X \sim$few$\times 10^{-2}$, after conversion of the quoted ionization parameter to that over the 0.1–10 keV band used here). Nandra et al (1997b) have recently reported the results from *ASCA* observations of the RQQ MR 2251-178 ($z = 0.068$, $L_X \simeq 2 \times 10^{45}$ erg s^{-1}), obtaining a lower column density ($N_{H,z} \sim 2 \times 10^{21}$ cm^{-2}) and $U_X \sim 0.07$. Brandt, Fabian & Pounds (1996) have found evidence for absorption by ionized oygen in *ROSAT* PSPC data from IRAS 13349+2438 ($z = 0.107$, $L_X \sim 10^{45}$–10^{46} erg s^{-1}). Unfortunately the properties of the ionized material could not be well constrained by those data ($N_{H,z} \sim$few$\times 10^{21}$–10^{24} cm^{-2}, $U_X \sim 0.2$–0.5). However, the lack of significant absorption by *neutral* material in the PSPC data along with strong evdience for dust at other wavebands led Brandt et al to suggest that the dust may be embedded within the ionized material.

A particularly interesting result of our analysis is the detection of an absorption feature within the Fe *K*-shell band (§3.2). The strength of this feature implies either an Fe/O

abundance ratio ~ 10 times cosmic, or a second zone of highly ionized material, perhaps outflowing from the nucleus. The feature is of similar energy and depth as those observed in Seyfert-I galaxies by *Ginga* (Nandra & Pounds 1994), and that possibly detected in an *ASCA* observation of the RLQ S5 0014+81 (Cappi et al 1997). Future observations, with higher sensitivity and resolution in the 7–9 keV band, are required to confirm these features and better determine their nature.

We would like to thank Keith Gendreau, Tahir Yaqoob, Tim Kallman, Smita Mathur, Bev Wills and Fred Hamann for useful discussions. We acknowledge the financial support of the Universities Space Research Association (IMG, TJT), National Research Council (KN) and Israel Science Foundation (NH). This research has made use of the Simbad database, operated at CDS, Strasbourg, France; of the NASA/IPAC Extragalactic database, which is operated by the Jet Propulsion Laboratory, Caltech, under contract with NASA; and of data obtained through the HEASARC on-line service, provided by NASA/GSFC.

REFERENCES

Arnaud, K.A., 1996, *Astronomical Data Analysis Software and Systems V* eds Jacoby, G., Barnes, J, p17, ASP Conf. Series vol 101.

Brandt, W.N., Fabian, A.C., Pounds, K.A., 1996, MNRAS, 278, 326

Burke, B.E., Mountain, R.W., Daniels, P.J., Dolat, V.S., 1994, IEEE Trans. Nuc. SCI. 41, 375

Cappi, M., Matsuoka, M., Comastri, A., Brinkman, W., Elvis, M., Palumbo, G.G.C., Vignali, C., 1997, ApJ, 478, 492

Dotani, T., et al., 1996, *ASCA News*, 4, 3

Fiore, F., Elvis, M., Mathur, S., Wilkes, B.J., McDowell, J.C., 1993, ApJ, 415, 129

Fiore, F., Elvis, M., Giommi, P., Padovani, P., 1997, ApJ, submitted

Gendreau, K., 1994, *ASCA News*, 2, 5

George, I.M., Turner, T.J., Netzer, H., Nandra, K., Mushotzky, R.F., Yaqoob, T., 1997, ApJS, submitted (G97)

Grandi, P., et al., 1997, A&A, in preparation

Halpern, J.P., 1984, ApJ, 281, 90

Laor, A., Fiore, F., Elvis, M., Wilkes, B.J., McDowell, J.C., 1994, ApJ, 435, 611

Laor, A., Fiore, F., Elvis, M., Wilkes, B.J., McDowell, J.C., 1997, ApJ, 477, 93

Makishima, et al 1996, PASJ, 48, 171

Mathur, S., 1997, in Proc. *Mass Ejection from AGN*, ed. Arav, N., Shlosman, I., Weyman, R., PASP, in press

Mineo, T., Stewart, G.C., 1993, MNRAS, 262, 817

Morrison, R., McCammon, D., 1983, ApJ, 270, 119

Murphy, E.M., Lockman, F.J., Laor, A., Elvis, M., 1996, ApJS, 105, 369

Nandra, K., Pounds, K.A., 1992, Nature, 359, 215

Nandra, K., Pounds, K.A., 1994, MNRAS, 268, 405

Nandra, K., George, I.M., Turner, T.J., Fukazawa, Y., 1996, ApJ, 464, 165

Nandra, K., George, I.M., Mushotzky, R.F., Turner, T.J., Yaqoob, T., 1997a, ApJ, 476, 70

Nandra, K., George, I.M., Mushotzky, R.F., Turner, T.J., Yaqoob, T., 1997b, in preparation

Netzer, H., 1993, ApJ, 411, 594

Netzer, H., 1996, ApJ, 473, 781

Ohashi, T., et al., 1996, PASJ, 48, 157

Pan, H.C., Stewart, G.C., Pounds, K.A., 1990, MNRAS, 242, 177

Reynolds, C.S., 1997, MNRAS, 286, 513

Schmidt, M., Green, R.F., 1983, ApJ, 269, 352

Serlemitsos, P.J., et al., 1995, PASJ, 47, 105

Turner, T.J., Nandra, K, George, I.M., Fabian, A.C., Pounds, K.A. 1993, ApJ, 419, 127

Williams, O.R., et al., 1992, ApJ, 389, 157

Table 1. Best-fitting spectral parameters to PG 1114+445

$N_{H,0}$ (10^{21} cm^{-2})	Γ	$N_{H,z}$ (10^{21} cm^{-2})	$\log U_X$	χ^2/dof	$\Delta\chi^2_{0.6}$	$\overline{R_{0.6}}$
ASCA analysis alone						
0.19 (f)	$1.75^{+0.10}_{-0.10}$	$19.60^{+4.39}_{-3.82}$	$-1.027^{+0.130}_{-0.162}$	478/504	10	0.8
$1.25^{+2.01}_{-1.06\ (p)}$	$1.78^{+0.15}_{-0.12}$	$21.03^{+11.33}_{-6.19}$	$-0.877^{+0.274}_{-0.280}$	475/503	6	1.2
Joint ASCA & ROSAT analysis						
$0.22^{+0.07}_{-0.03\ (p)}$	$1.79^{+0.12}_{-0.10}$	$22.94^{+5.57}_{-4.28}$	$-0.922^{+0.111}_{-0.084}$	508/539	31	0.6
0.19 (f)	$1.76^{+0.06}_{-0.07}$	$21.42^{+3.80}_{-2.64}$	$-0.953^{+0.107}_{-0.105}$	508/540	23	0.7

Note. — Fits undertaken in the 0.6–10.0 keV and 0.1–2.0 keV bands in the observer's frame for *ASCA* and *ROSAT* respectively. $N_{H,0}$ is the neutral column at $z = 0$ (constrained to be $\geq N_{HI}^{Gal} = 1.94\times10^{20}$ cm^{-2}); Γ is the photon index of the underlying powerlaw continuum; $N_{H,z}$ is the column density of the ionized gas at the redshift of the source; U_X is ionization parameter (see text); $\Delta\chi^2_{0.6}$ is the increase in the χ^2-statistic, $\overline{R_{0.6}}$ the mean data/model ratio when the best-fitting model is extrapolated to the 6 SIS spectral bins < 0.6 keV. The errors are at 68% confidence for 3 (lines 1 & 3) and 4 (lines 2 & 4) interesting parameters. (f) indicates the parameter was fixed at the specified value, and (p) that $N_{H,0}$ 'pegged' at N_{HI}^{Gal}.

Table 2. Derived column densities of Li-like ions for $U_X = 0.1$, $N_{H,z} = 2 \times 10^{22}$ cm^{-2}

ion	N_{ion} (cm^{-2})
CIV	3.1×10^{14}
NV	3.9×10^{15}
OVI	4.5×10^{17}
NeVIII	5.0×10^{17}
MgX	2.9×10^{17}
SiXII	1.4×10^{17}
SXIV	9.9×10^{15}
ArXVI	1.4×10^{14}

Note. — It should be stressed that the predicted column densities are very sensitive to form of the ionizing continuum in the XUV band, and of course the elemental abundances (see §4).

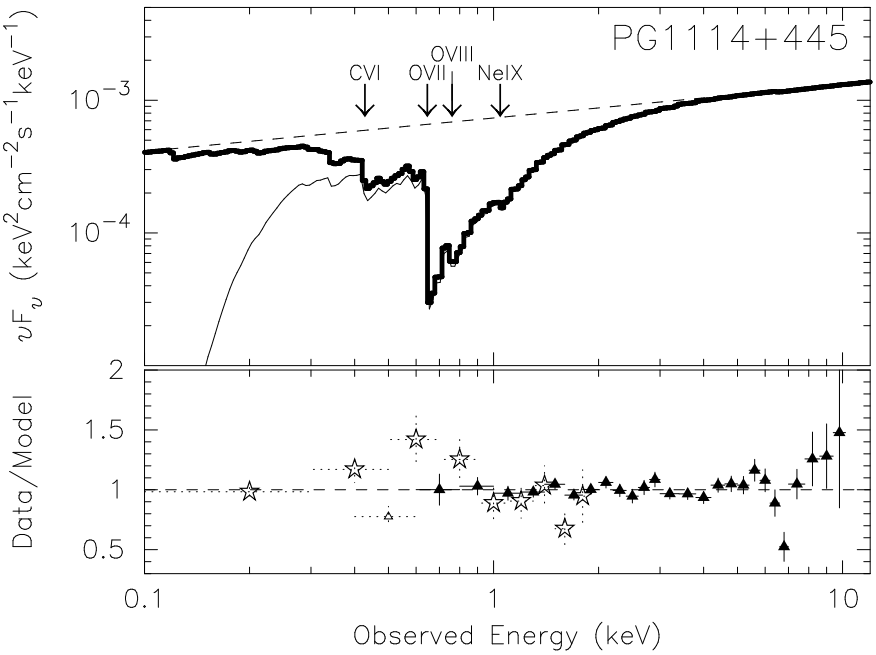

Fig. 1.— Upper panel: The preferred ionized-absorber model for PG 1114+445 based on the *ASCA* observations performed in 1996 Jun. The dashed line shows the underlying powerlaw continuum, the bold curve shows the best-fitting spectrum (corrected for Galactic absorption with $N_{HI}^{Gal} = 1.94 \times 10^{20}$ cm^{-2}) the faint solid line shows the observed spectrum (uncorrected for N_{HI}^{Gal}). The deep absorption features due to CVI, OVII and OVIII are clearly visible in the spectrum, as is the fact that the ionized gas becomes transparent below ~ 0.4 keV. The preferred model has an ionization parameter $U_X \simeq 0.1$, and an effective hydrogen column denisty $N_{H,z} \simeq 2 \times 10^{22}$ cm^{-2} assuming abundances relative to hydrogen of $A_{\rm C} = 3.7 \times 10^{-4}$, $A_{\rm O} = 8 \times 10^{-4}$ and $A_{\rm Ne} = 1.1 \times 10^{-4}$ for C, O and Ne respectively. Lower panel: the mean data/model ratio from this fit (where, for clarity, we show the rebinned, averaged ratios for *ASCA*). The filled triangles correspond to the *ASCA* data used during the spectral analysis, whilst the open triangle shows the ratio when the best-fitting model is extrapolated < 0.6 keV in the SIS. The open stars show the corresponding data/model ratio (again rebinned for clarity) when this model is *directly compared* to the *ROSAT* PSPC data.

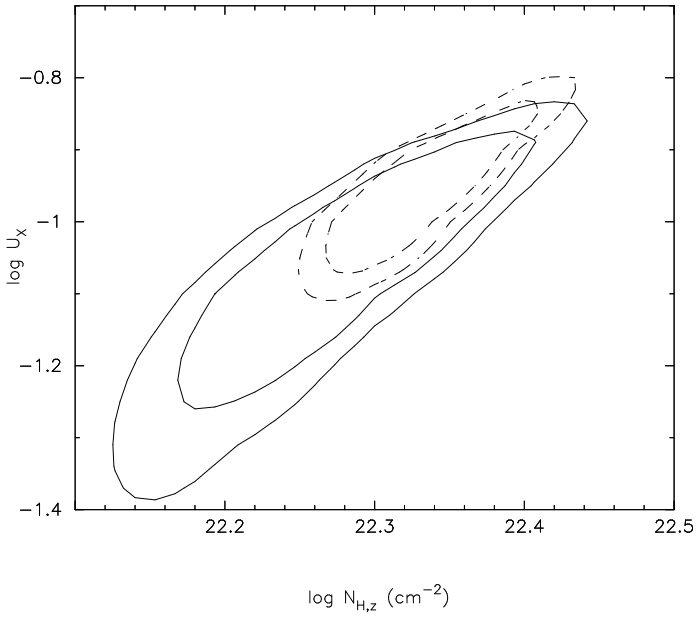

Fig. 2.— χ^2 contours corresponding to the 68 and 95% confidence regions (for 3 interesting parameters: Γ, U_X & $N_{H,z}$) from the *ASCA* analysis alone (solid curves) and the analysis of the joint *ASCA*/*ROSAT* analysis (dashed curves). Clearly both analyses are consistent with an X-ray ionization parameter $U_X \simeq 0.1$ and column density $N_{H,z} \simeq 2 \times 10^{22}$ cm^{-2}.

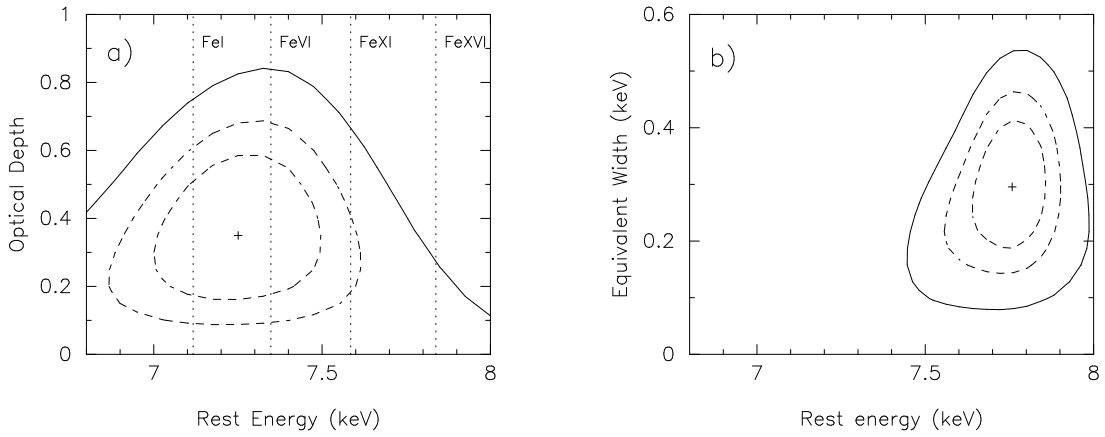

Fig. 3.— a) The dashed curves show the χ^2 contours corresponding to the 68 and 90% confidence regions for 2 interesting parameters (E_z^{abs} & τ), when an additional absorption edge is added to ionized-absorber model described in §3.1. The solid curve shows the contour corresponding to 90% confidence for 5 interesting parameters (Γ, U_X, $N_{H,z}$, E_z^{abs} & τ). As can be seen, such a feature is consistent with a variety of ionization states of iron up to ∼FeXIX. b) As above, but for when the 'notch'-shaped absorption feature is added to ionized-absorber model. Such a feature is consistent with resonance scattering by Ni $K\alpha$ (<NiXXVIII) and Fe $K\beta$ (>FeXX) in the rest–frame of the quasar or Fe $K\alpha$ in out-flowing material (see §3.2).